Special issue mini-review

MRC

Received: 30 June 2014 Revised: 17 December 2014 Accepted: 19 January 2015 Published online in Wiley Online Library: 9 April 2015

(wileyonlinelibrary.com) DOI 10.1002/mrc.4220

New applications and perspectives of fast field cycling NMR relaxometry

Rebecca M. Steele,[a]* Jean-Pierre Korb,[b] Gianni Ferrante[a] and Salvatore Bubici[a]

The field cycling NMR relaxometry method (also known as fast field cycling (FFC) when instruments employing fast electrical switching of the magnetic field are used) allows determination of the spin-lattice relaxation time (T_1) continuously over five decades of Larmor frequency. The method can be exploited to observe the T_1 frequency dependence of protons, as well as any other NMR-sensitive nuclei, such as ^{2}H, ^{13}C, ^{31}P, and ^{19}F in a wide range of substances and materials. The information obtained is directly correlated with the physical/chemical properties of the compound and can be represented as a 'nuclear magnetic resonance dispersion' curve.

We present some recent academic and industrial applications showing the relevance of exploiting FFC NMR relaxometry in complex materials to study the molecular dynamics or, simply, for fingerprinting or quality control purposes. The basic nuclear magnetic resonance dispersion features are outlined in representative examples of magnetic resonance imaging (MRI) contrast agents, porous media, proteins, and food stuffs.

We will focus on the new directions and perspectives for the FFC technique. For instance, the introduction of the latest Wide Bore FFC NMR relaxometers allows probing, for the first time, of the dynamics of confined surface water contained in the macro-pores of carbonate rock cores.

We also evidence the use of the latest field cycling technology with a new cryogen-free variable-field electromagnet, which enhances the range of available frequencies in the 2D T_1–T_2 correlation spectrum for separating oil and water in crude oil. **Copyright © 2015 John Wiley & Sons, Ltd.**

Keywords: NMR; relaxometry; fast field cycling relaxometry; T_1; NMRD; molecular dynamics; low-field NMR; TD NMR

Introduction

As the designer of instruments and methods for fast field cycling (FFC) NMR relaxometry, we intend to acknowledge, in this mini review, some of the many recent applications of this variant of the field cycling (FC) NMR relaxometry technique and how the research has evolved, including some of the more recent discoveries made using FFC. We will discuss how FFC instruments are evolving and how this will help the development of new applications in academia and accommodate requirements for industrially important applications.

Field cycling NMR relaxometry is the only low-field NMR technique that measures the longitudinal spin relaxation rate, $1/T_1$, as a function of the magnetic field strength, over a wide range of frequencies (from a few kilohertz to 42 MHz (1 T) or higher with the limitation being the size of the magnet and the FC technique being used – see succeeding text), corresponding to values of T_1 in the order of seconds to a fraction of a millisecond. This can be carried out by using a single instrument with a magnet capable of fast electrical switching of the field (thus also known as FFC), which is commercially available (vide infra), or through home-built systems, which involve physically moving the sample between different magnets or within the stray magnetic field of a high field magnet, known as 'shuttling'.[1–6] The data can be displayed in the form of a nuclear magnetic resonance dispersion (NMRD) profile, $R_1(\omega_0) = 1/T_1(\omega_0)$ *versus* the Larmor frequency $\omega_0/2\pi$.[1,7] A typical example is displayed in Fig. 1 that represents the NMRD response of a Gd^{3+} contrast agent when free in solution and bound to a protein.[8]

Commercial FFC NMR relaxometers, which have been around since 1997 (see Fig. 2), exploit the principle that the nuclear spin-lattice relaxation, T_1, is dependent on the magnetic field strength, as discovered in very early works[9,10] and allow an NMRD profile to be obtained quickly without changing instruments due to the fast electronic switching time, in the order of 150 μs. In comparison, FC methods using mechanical shuttling have sample shuttling times in the order of 100 ms and thus have a restricted applicability to correspondingly longer T_1 relaxation times.[1–4,6] FFC technology has improved significantly since the first version of the SPINMASTER FFC 0.5T relaxometer, from Stelar s.r.l. (Mede, Italy), was installed at the University of Lund in 1997. This NMR relaxometer incorporated a two-layer air-core solenoid magnet capable of achieving magnetic field strengths, by fast electrical switching, from 10 kHz to 20 MHz. The more compact higher performance version of the SPINMASTER was launched in the year 2000 with a 1T four-layer air-core solenoid magnet, capable of achieving fields from a few kilohertz (1–10 kHz is achievable depending on the local environment and field) to 42 MHz, with improved switching times. The current SPINMASTER instrument is undergoing further improvements

* *Correspondence to: Rebecca M. Steele, Stelar s.r.l., Via E. Fermi 4, 27035 Mede, PV, Italy. E-mail: steele@stelar.it*

a *Stelar s.r.l., Via E. Fermi 4, 27035 Mede, PV, Italy*

b *Physique de la Matière Condensée, Ecole Polytechnique-CNRS, 91128 Palaiseau, France*

 Copyright © 2015 John Wiley & Sons, Ltd.

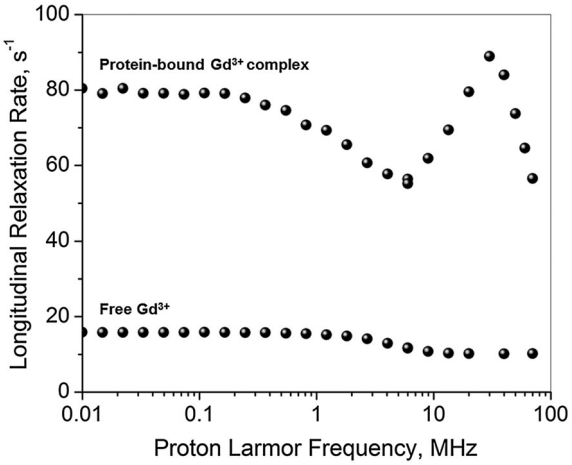

Figure 1. Example of ^{1}H NMRD profiles for a Gadolinium(III) complex bound to a protein and free in solution. To obtain a good NMRD profile $1/T_1$ was measured at more than 20 different magnetic field strengths between 10 kHz and 100 MHz. Note that binding of the paramagnetic nucleus to a protein causes and increase in the relaxation, which is a desirable property of a contrast agent.

for the performance, and a new configuration, in the form of a 0.5T wide bore magnet for 1-inch samples, has been introduced, which will be discussed in the section on new perspectives. The development, which made FFC relaxometry accessible to more researchers and especially to industry, was the advent of the bench-top FFC relaxometer from Stelar in 2006, known as the SMARtracer. This compact 0.25T FFC relaxometer allows the nuclear spin-lattice relaxation rate, $1/T_1$, of solid or liquid samples in a 10-mm standard NMR tube, to be measured within the field range of few kilohertz to 10 MHz.

Discussion

Generally, the benefit of exploring the nuclear spin-lattice relaxation rate, $1/T_1$, over a large range of frequencies is to isolate the typical NMRD dispersion features associated with the different processes of molecular dynamics. Varying the magnetic field changes the Larmor frequency ($\omega_0 = \gamma B_0$ where γ is the gyromagnetic ratio) and therefore the time and length scales of the fluctuations responsible for the nuclear spin-lattice relaxation rate $1/T_1$. This is especially true in spatially confined systems that force more frequent re-encounters between bulk proton (or other nuclei such as ^{19}F,[11,12] ^{31}P,[13] ^{2}H,[14] ^{7}Li,[15] and ^{13}C[16–18]) species and any other nuclei present at a particular solid–liquid interface.[19,20] However, the FFC technique can also be applied to bulk liquids.[1] Effectively, it is possible to measure almost any material, solid, liquid, colloid, or complex mixture using NMRD, although as it will be explained in the succeeding text, there are certain areas of application where this technique is notably more effective and useful in providing information on the molecular dynamics (actual or changing) of the substance being measured.

Some representative examples of the problems addressed by researchers are fluid dynamics at the solid interface, transport in porous media (filtration, imbibition, and conduction),[21] role of physical chemistry at the pore surface (proton exchange and wettability),[22,23] phase transitions in confinement, hydration of proteins, biological tissues and membranes,[24–28] dynamics of water at the protein surface,[29–35] dynamics of polymers[36–41] and liquid crystals,[12,42–45] and the study of MRI contrast agents and differential diagnosis.

Examples of some of the problems addressed by the industry are durability of cements and concretes,[12,46–48] determination of oil to water ratios in rock cores,[23] filtration and water purification in soils,[49–52] chemical reactivity (catalysis),[53] aging and

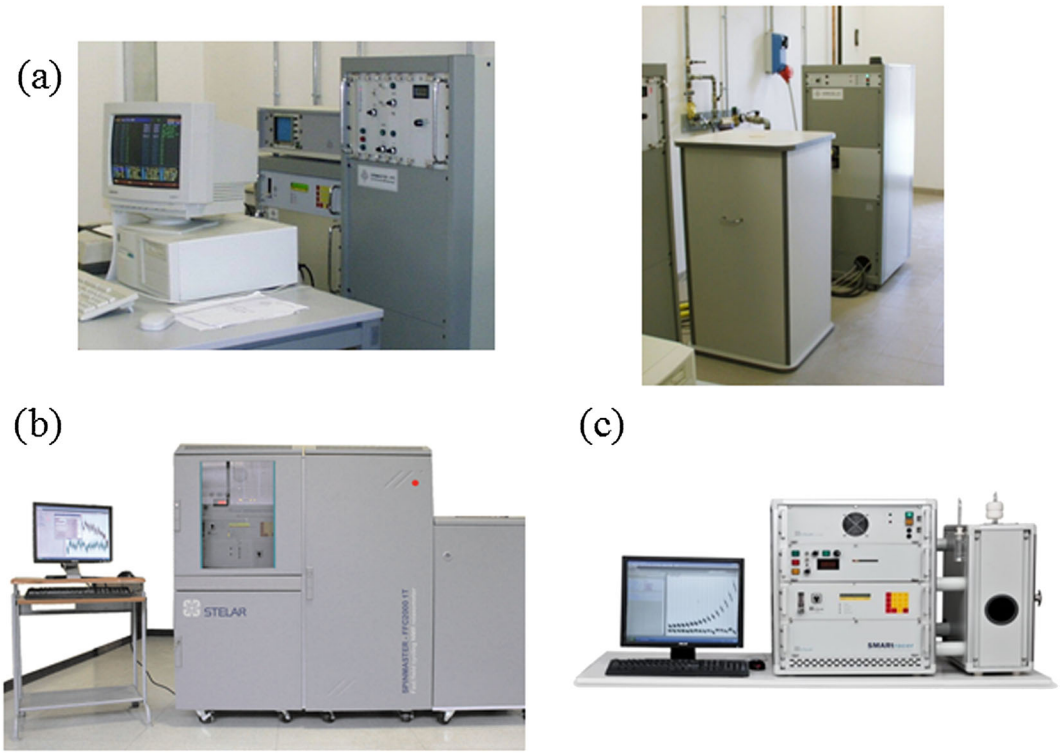

Figure 2. Commercial FFC relaxometers (a) the first version of the SPINMASTER 0.5 T, installed at the University of Lund, Sweden, in 1997; (b) SPINMASTER 1T FFC 2000 – revision of the instrument led to a more powerful and compact version; (c) the bench-top 0.25T SMARtracer launched in 2006.

 Copyright © 2015 John Wiley & Sons, Ltd.

spoilage of complex food substances,[54,55] and quality control and anti-fraud controls.[56]

Returning to the classical example of Gadolinium-based paramagnetic contrast agents[8] (an example of a classical NMRD profile is shown in Fig. 1), this is one area of medical research where rapid progress has been made, in both the type and chemical conformation of the agent as well as in the instrument technology to characterize the T_1 relaxivity profile (NMRD) of the agent (contrast agents with higher relaxivity are more desirable as they tend to enhance the relaxation of body tissues of interest in the MRI scan). Research on contrast agents has led, importantly, to the development of MRI-trackable magnetic nanoparticles, capable of targeting specific cell types, such as cancer cells, for image-guided treatment.[57–59] The size of the magnetic nanoparticles is important, and NMRD profiles are able to relay important dynamics information on these. For example, Fig. 3 shows that increasing the core size of the iron-based nanoparticles from 4 to 14 nm causes a desired increase in relaxivity ($mM^{-1}\,s^{-1}$).

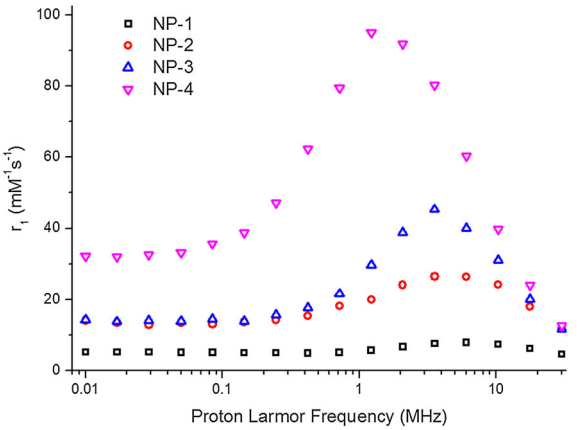

Figure 3. ^{1}H NMRD profiles of magnetic iron oxide nanoparticles with increasing core sizes: 4 nm (NP-1, black squares), 6 nm (NP-2, red circles), 9 (NP-3, blue upward-pointing triangles), and 14 nm (NP-4, pink downward-pointing triangles).

Indeed, in the ambient of clinical and pre-clinical research, FFC experiments can also be compared with 'rotating frame' experiments, which give similar but more limited information. The rotating frame experiments rely on the B_1 excitation field, which allows measurement of the NMRD in a limited but complementary low frequency range. For example, the spin-lattice relaxation time, T_1, in the rotating frame ($T_{1\rho}$), was quantified for various clinical grades of human osteoarthritis (OA), by measuring cartilage specimens obtained from total knee replacement surgery. The $T_{1\rho}$ was compared

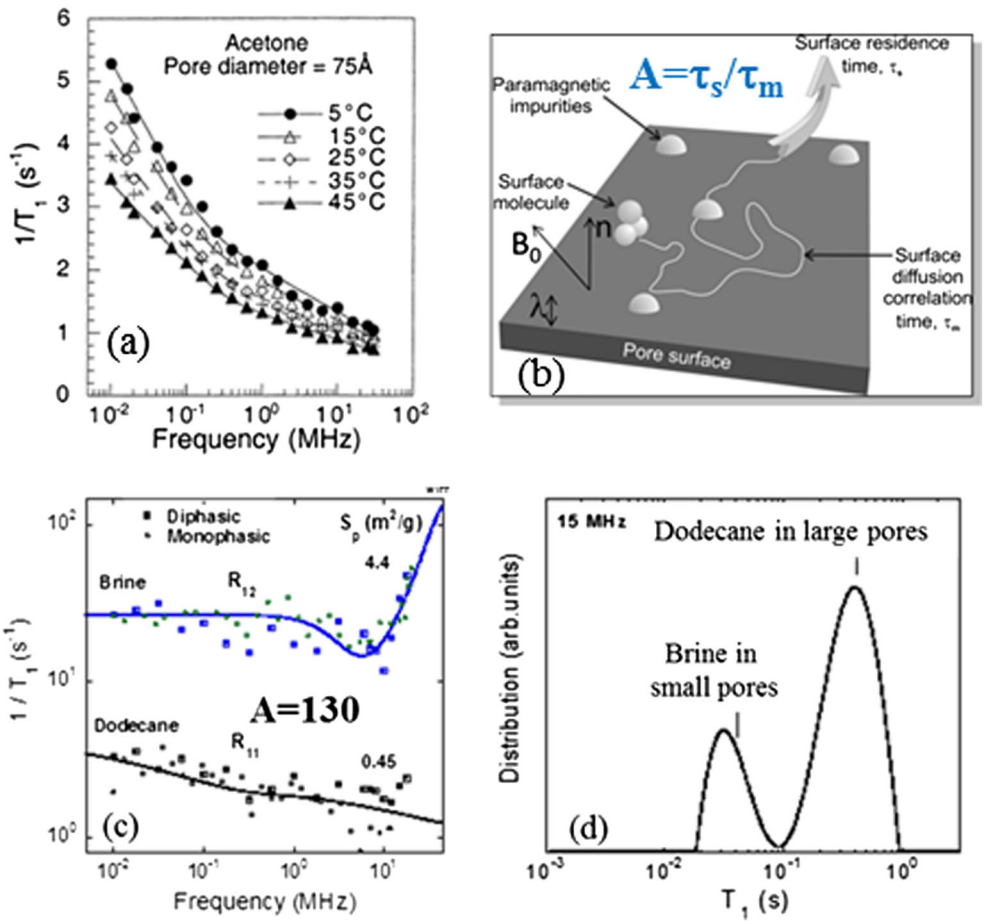

Figure 4. (a) ^{1}H NMRD profiles of aprotic acetone in controlled pore chromatographic glass purchased from Sigma Chemical Company micro-pores of average pore diameter of 75 Å that have paramagnetic ion impurities at the level of 40 ppm at different temperatures.[61] (b) The continuous lines that represent the best fits achieved with a bi-logarithmic surface diffusion relaxation model is described. (c) The very different ^{1}H NMRD profiles observed in carbonate rock cores show that water stays bound in small pores, whereas oil (dodecane) diffuses at the surface of large pores.[23] (d) The quantitative analysis of the NMRD shown in (c) allows the assignment of water and oil in the bimodal T_1 distribution observed at 15 MHz.

Copyright © 2015 John Wiley & Sons, Ltd.

with the transverse relaxation time (T_2) and correlated with the OA disease progression.[60]

One of the most successful examples of application of NMRD is related to probing the molecular dynamics specifically on the internal surfaces of multi-scale porous media. Here, the biphasic fast exchange model favors, on the time scale of an NMR experiment, the fast molecular exchange between the slow (e.g. 2.5 s) and the fast (e.g. 5 ms) relaxing protons of bulk water and water at the pore surface, respectively. For example, Fig. 4a shows the NMRD profiles, at different temperatures, of an aprotic but polar liquid (acetone) diffusing in the proximity of Fe^{3+} paramagnetic ions fixed on the pore surface of a calibrated porous material (pore diameter of 7.5 nm).[61] The observed bi-logarithmic frequency dependence, which is commonly observed in these materials, is due to a surface relaxation model described in Fig. 4b where one introduces a translational correlation time τ_m to describe the molecular surface diffusion and a time of residence τ_s of the moving proton spins on the pore surface. The ratio of these two measured correlation times $A = \tau_s/\tau_m$ thus becomes a molecular indicator of the dynamical surface affinity of the embedded liquid. It also represents the local NMR wettability in pores. Figure 4c and 4d shows that it is possible to extend the FFC technique to separate oil and water in the complex pore network of real carbonate rock cores from their very different NMRD profiles in rock cores.[23] This is critical in understanding the quantity of oil held in the rock, and the best methods of oil extraction also depend on this and the type of rock (the porosity, pore size distribution, and wettability).[19–23] It is also possible to use NMRD to study the levels of unwanted asphaltene aggregates in crude oils. Asphaltene is considered as a poison in the oil industry as it clogs the pores of the rocks from which the oil is extracted, thus lowering the yield of crude oil.[62,63]

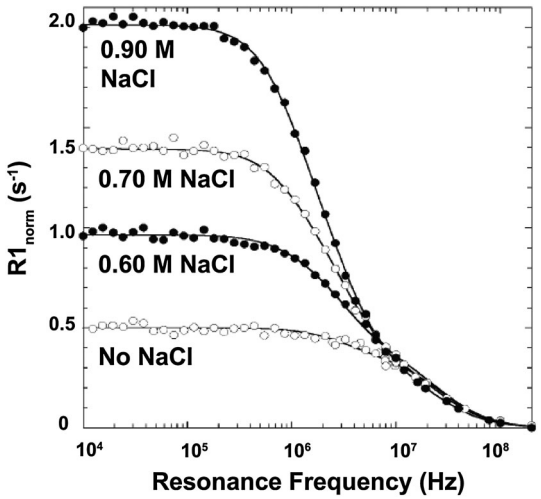

Figure 5. ^{1}H NMRD profiles of aqueous solutions of BPTI at different concentrations of NaCl reported in the diagram at 27 °C, and pH 4.5. $1/T_1$ measurements were carried out from 10 kHz to 200 MHz.[64]

Nuclear magnetic resonance dispersion has also been used successfully to study the dynamics of water on the surface of proteins.[30–35] Proteins being large macromolecules are perfect candidates for dynamics studies through NMRD as they tend to rotate slowly, and the low field strengths achievable on FFC relaxometers can capture these slow motions. Proteins have a tendency to aggregate, and NMRD profile changes in correlation to the size of the aggregate. Figure 5 shows how the sodium chloride salt concentration affects aggregation of the protein bovine pancreatic trypsin inhibitor (BPTI). More decamers of the BPTI form as the salt concentration increases.[64] It is also possible to use the quadrupolar dips found in the NMRD of proteins, due to cross relaxation of the ^{1}H and ^{14}N nuclei,[65] to understand the concentration of fibrin, for example, which could be useful for classification of thrombi in medicine.[66] The FFC technique could indeed be a valuable addition to the array of methods currently used to study proteins.

Figures 6 and 7 show how NMRD could be applied in the food industry to study aging and spoilage of food for shelf life. Figure 6a shows how the NMRD profile of a piece of fresh banana changes over a period of 20 h, and Fig. 6b shows how the T_1 varies largely from very low magnetic field strengths (0.01 MHz) to the higher field strengths (20 MHz). Figure 7 shows how the NMRD profiles of an unspoiled milk-based refrigerated drink product, within its expiry date, and a sample of the same product after induced spoilage change especially at the lower magnetic field strengths.[67]

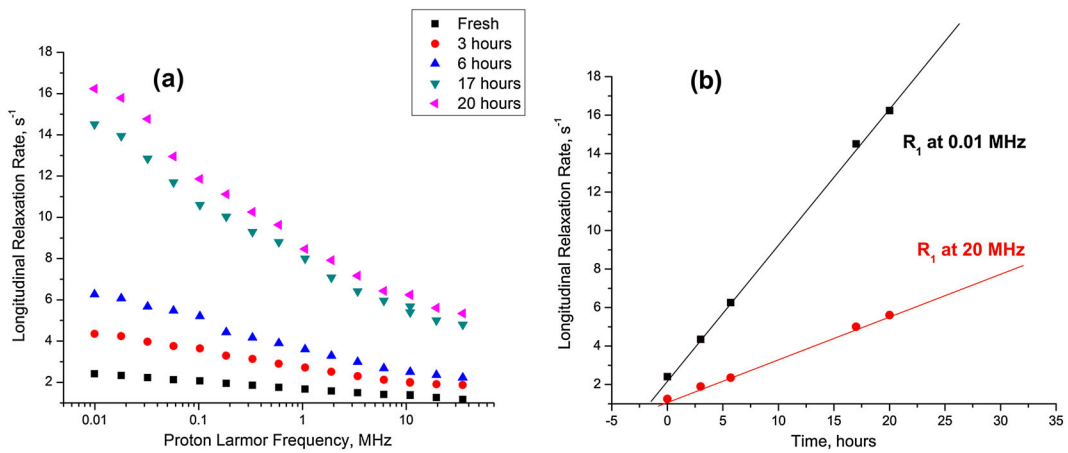

Figure 6. (a) ^{1}H NMRD profiles of a piece of banana were measured as a function of the time with the aim to monitor the aging effects. $1/T_1$ of the banana was measured when freshly opened (black squares), then after exposed to air re-measured after 3 (red circles), 6 (blue triangles), 17 (green downward-pointing triangles), and 20 h (pink-skewed triangles) at 15 different magnetic field strengths between 10 kHz and 42 MHz. (b) R_1 of the banana varies with magnetic field strength and over time. At 0.01 MHz, R_1 fits the aging process with a larger gradient than at 20 MHz, and thus, it is more advantageous to use lower field strengths for such applications with a view to quality checks.

Copyright © 2015 John Wiley & Sons, Ltd.

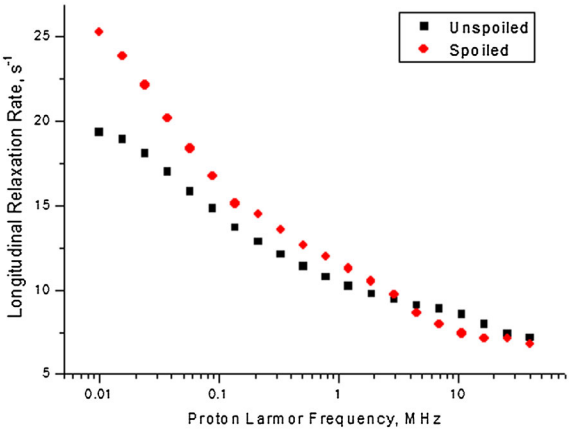

Figure 7. ^{1}H NMRD profiles of an unbranded milk-based refrigerated drink product in its original state, within expiry date (unspoiled, black squares), and after induced spoilage (spoiled, red diamonds). $1/T_1$ was measured for each sample at 20 different magnetic field strengths between 10 kHz and 42 MHz.

Indeed, the NMRD profile is able to give information such as identifying the contributions of different phases (solid–liquid and water–fat),[54,68] understanding distribution of moisture throughout a food matrix,[69] to help define shelf life,[54,55] showing particular characteristics of products of denominated or geographic origin[70] for anti-fraudulent purposes,[56] or may be simply employed as a method to fingerprint a product for quality control purposes.

New perspectives of FFC relaxometry

For a long time, an important demand of industrial partners on FFC relaxometry was to drastically enlarge the size of the sample studied. This is indeed the case for petroleum industry where the usual rock cores reach 1 inch in diameter.

The most recent introduction of the latest Wide Bore FFC NMR relaxometers has allowed the dynamics of confined surface water contained in the pores of rock cores, of representative sizes, to be probed for the first time. A 40-mm bore FFC magnet with a 0.45T maximum polarizing field has proven useful to study different carbonate rock samples (25 mm in diameter and 20 mm in height), with different porosities, saturated with deionized water (Fig. 8).[71]

For each sample of carbonate rock, we observed the evolution of a highly skewed T_1 distribution (Fig. 9a) with the Larmor frequency. Through ESR spectroscopy, we found that Mn^{2+} was the source of relaxation in the NMRD of the water embedded in the rock cores studied. The bi-logarithmic behavior observed here (Fig. 9b) is again because of the reduced dimensionality of the local water dynamics that enhances drastically the re-encounter probability between protons in the water and Mn^{2+} spins that maintain the pairwise dipolar correlation between these two spins for a long time (low frequency). We succeeded in probing the microscopic dynamical surface affinity, $A = \tau_s/\tau_m$, in lieu of the more traditional and loosely defined macroscopic wettability indices. This index A represents roughly the average number of diffusing steps of water protons in the proximity of fixed paramagnetic Mn^{2+} sites during the time scale of an NMRD measurement. We show in Fig. 9b that this local NMR wettability depends critically on the pore sizes.[71]

The new wide bore FFC magnet technology can also be exploited in many other studies where observation of large volume samples is necessary. Indeed, the same 40-mm wide bore FFC magnet has been recently introduced to allow the acquisition of T_1-weighted MRI images at different magnetic fields by offsetting magnetic field of a clinical MRI scanner.[72]

Two-dimensional relaxation mapping (in the form of T_1–T_2 spin correlation spectra) has been used previously for the study of proton exchange, diffusion, and pore geometry in porous materials at one fixed field strength. One such example is the NMR measurements of low field relaxation and diffusion that were performed in the fringe field of a horizontal bore of a 2T magnet at 5.03 MHz. This technique measured the 2D distribution functions $f(D,T_2)$ and $f(T_1, T_2)$ for different classes of crude oils in the presence and absence of asphaltene molecules.[73,74]

It is now possible to obtain 2D T_1–T_2 spin correlation spectra with FFC, providing that the Carr-Purcell Meiboom-Gill (CPMG)

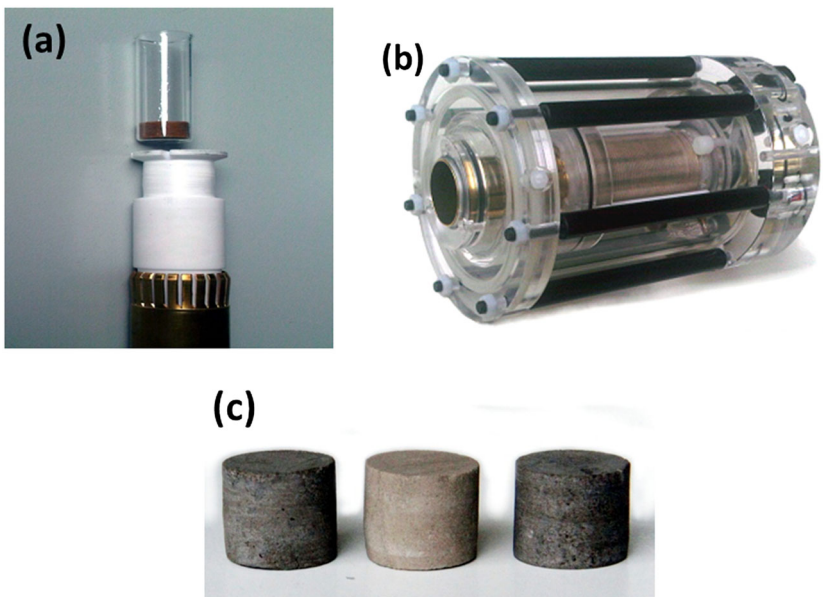

Figure 8. (a) Large volume NMR probe (Stelar). (b) Wide bore FFC 0.45T magnet (Stelar). (c) Three samples of carbonate rocks, measuring 25 mm in diameter and 20 mm in height, with different porosity, saturated with deionized water (S40, S50, and S122).

 Copyright © 2015 John Wiley & Sons, Ltd.

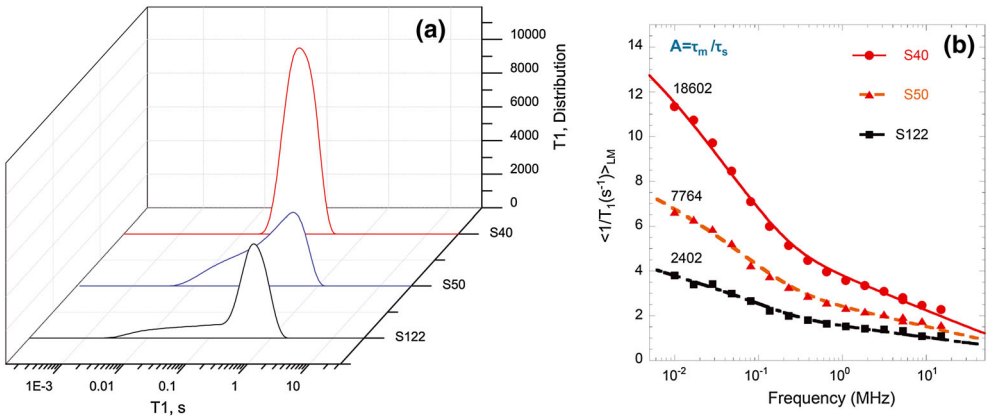

Figure 9. (a) T_1 distributions of three carbonate rock core samples (from Fig. 8c) at 0.01 MHz. As the T_1 distributions of the three studied samples are different in shapes, it is absolutely necessary to consider the logarithmic average $<1/T_1>$ for a meaningful interpretation of the NMRD. (b) Nuclear magnetic relaxation dispersion of the logarithmic average $<1/T_1>$ of the three rock cores. The consideration of such a logarithmic average thus allows quantitative comparison of the different NMRD data of the three samples. The continuous lines are the best fits obtained with a bi-logarithmic surface relaxation model. The dynamical surface affinity index, *A*, representing the local NMR wettability is given above each fit.

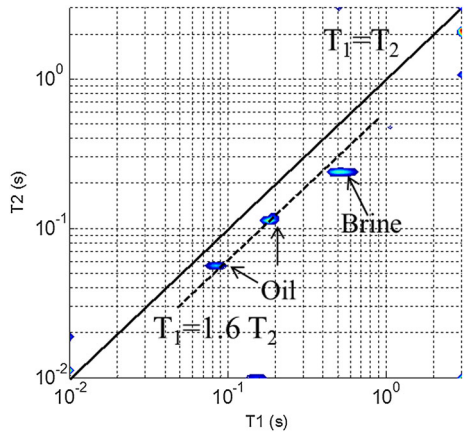

Figure 10. T_1–T_2 correlation spectrum of a mixture of bulk water and crude oil pools obtained at 30 MHz on a 5T cryogen-free variable-field electromagnet (HTS-110) connected to a PC-NMR FFC console (Stelar). The continuous line represents the line $T_1 = T_2$ characteristics of a single bulk phase. The dashed line shows the best fit of the results $T_1 = 1.6\,T_2$, typical of a surface diffusion between the different proton species of oil and brine-labeled as shown by the arrows in the diagram.

T_2measurements are made at the detection frequency. This will help in separating the contribution of separated fluids in porous media. Indeed, further work toward this objective is now in progress.

In multi-component systems, there is potentially an exchange of proton magnetization between the various proton pools. This can occur by proton exchange and dipolar cross relaxation, which introduces exchange cross-peaks into the 2D T_1–T_2 spectrum.[75] The extension to two dimensions has succeeded in resolving many more peaks. However, it could be necessary to vary the magnetic field for proper assignment of the different peaks. Mixing the FFC technique with a new cryogen-free variable-field electromagnet (from HTS-110, New Zealand) enhances the range of available frequencies thus allowing the separation of oil and water in crude oil.[71] In Fig. 10, we show that the 2D T_1–T_2 plots of a mixture of bulk water and crude oil pools do not reveal any exchange between the different and independent pools. The quantitative analysis of the peak intensities thus gives information on the relative populations of the two fluids. This method could be important for analyzing in real time the quantity of water in crude oil.

Indeed, a new recent study on the dynamics and wettability of oil and water in shale rocks has confirmed that using NMRD combined with T_1–T_2 mapping methods, it is possible to separate out and assign the contributions of oil and water in a confined porous system and thus provide an invaluable tool for investigating the oil and gas recoveries in these important porous rocks.[76]

Another recently notable enhancement to the FFC technique has been reported for ^{13}C FFC relaxation measurements: the NMRD of ^{13}C can be dramatically enhanced by using dynamical nuclear polarization, especially in polymer systems.[16,18]

Conclusions

In this article, we have outlined some of the more recent applications of FFC relaxometry methods for solving problems in academic and industrial contexts.

The study of NMRD profiles of protons and other important NMR-sensitive nuclei can offer unique insights, not available with any other NMR techniques, for the comprehension of molecular dynamics of complex matrices.

A non-conventional instrumental platform, suitable for multi-frequency NMR relaxometry, is now available for the investigation of different sample specimens in porous media, polymers, food, proteins, and biological tissues.

Indeed, the new generation of FFC relaxometers allows NMRD profiles to be obtained over a much larger range of Larmor frequencies and with much larger, more representative samples than before. With the latest instrumental development, it is also possible to obtain 'field-dependent' 2D T_1–T_2 correlation spectra, which in the petroleum industry would permit the quantitative separation of a mixture of crude oil and water.

Developments are also ongoing to combine the FFC technique with hyperpolarization methods such as DNP, which will drastically enhance the sensitivity of ^{13}C and will allow the measurement of ^{13}C-NMRD in polymers and proteins.

In conclusion, the FFC technology is now at a level of sophistication and maturity where industrial applications are possible. An important challenge is the transfer of this technique to industry and unexplored economic sectors.

 Copyright © 2015 John Wiley & Sons, Ltd.

Acknowledgements

The authors wish to thank all the technical staff at Stelar (past and present) involved in the development and production of Stelar FFC relaxometers, A. Boni ('Istituto Italiano di Tecnologia Center for Nanotechnology Innovation @NEST', Pisa, Italy) for providing samples of iron oxide nanoparticles for FFC relaxometric measurements in Fig. 3, P. Fantazzini and V. Bortolotti (University of Bologna) for the stimulating discussions and support in preparing the carbonate rock samples, and D. Pooke and M. Mallett at HTS-110 (Lower Hutt, New Zealand) for collaboration and use of the 200-MHz cryogen-free variable-field electromagnet for T_1–T_2 measurements on oil and water.

References

[1] R. Kimmich, E. Anoardo. *Prog. Nucl. Magn. Reson. Spectrosc.* **2004**, *44*, 257–320; DOI: 10.1016/j.pnmrs.2004.03.002.
[2] A. G. Redfield. *Magn. Reson. Med.* **2003**, *41*, 753–768; DOI: 10.1002/mrc.1264.
[3] A. G. Redfield. *J. Biomol. NMR* **2012**, *52*, 159–177; DOI: 10.1007/s10858-011-9594-1.
[4] C. Job, J. Zajicek, M. F. Brown. *Rev. Sci. Instrum.* **1996**, *67*, 2113–2122; DOI: 10.1063/1.1147024.
[5] S. Wagner, T. R. J. Dinesen, T. Rayner, R. G. Bryant. *J. Magn. Reson.* **1999**, *140*, 172–178; DOI: 10.1006/jmre.1999.1811.
[6] K. Victor, V. Kavelius, R. G. Bryant. *J. Magn. Reson.* **2004**, *171*, 253–257; DOI: 10.1016/j.jmr.2004.08.025.
[7] G. Ferrante, S. Sykora, in *Advances in Inorganic Chemistry*, vol. *57* (Eds: R. van Eldik, I. Bertini), Elsevier, New York, **2005**, pp. 406–466.
[8] E. Gianolio, G. B. Giovenzana, D. Longo, I. Longo, I. Menegotto, S. Aime. *Chem. Eur. J.* **2007**, *13*, 5785–5797; DOI: 10.1002/chem.200601277.
[9] N. F. Ramsey, R. V. Pound. *Phys. Rev.* **1950**, *77*, 278–279.
[10] A. Abragam, *The Principles of Nuclear Magnetism*, Clarendon Press, Oxford, **1961**.
[11] A. B. Koudriavtsev, M. D. Danchev, G. Hunter, W. Linert. *Cement Concr. Res.* **2006**, *36*, 868–878; DOI: 10.1016/j.cemconres.2005.09.015.
[12] S. Bubici, L. Calucci, G. Ferrante, M. Geppi. *Chem. Phys. Lett.* **2012**, *549*, 27–31; DOI: 10.1016/j.cplett.2012.08.031.
[13] M. F. Roberts, A. G. Redfield. *J. Am. Chem. Soc.* **2004**, *126*, 13765–13777; DOI: 10.1021/ja046658k.
[14] G. Schauer, R. Kimmich, W. Nusser. *Biophys. J.* **1988**, *53*, 397–404; DOI: 10.1016/S0006-3495(88)83116-3.
[15] M. Graf, B. Kresse, A. F. Privalov, M. Vogel. *Solid State Nucl. Magn. Reson.* **2013**, *51-52*, 25–30; DOI: 10.1016/j.ssnmr.2013.01.001.
[16] P. Miéville, S. Jannin, G. Bodenhausen. *J. Magn. Res.* **2011**, *210*, 137–140; DOI: 10.1016/j.jmr.2011.02.006.
[17] N. Chattergoon, F. Martínez-Santiesteban, W. B. Handler, J. H. Ardenkjaer-Larsen, T. J. Scholl. *Contrast Media Mol. Imaging* **2013**, *8*, 57–62; DOI: 10.1002/cmmi.1494.
[18] O. Neudert, H. P. Raich, C. Mattea, S. Stapf, K. Münnemann. *J. Magn. Reson.* **2014**, *242*, 79–85; DOI: 10.1016/j.jmr.2014.02.001.
[19] J.-P. Korb. *Magn. Reson. Imaging* **2001**, *19*, 363–368; DOI: 10.1016/S0730-725X(01)00249-1.
[20] S. Muncaci, C. Mattea, S. Stapf, I. Ardelean. *Magn. Reson. Chem.* **2013**, *51*, 123–128; DOI: 10.1002/mrc.3924.
[21] J.-P. Korb, in *Fluid Transport in Nanoporous Materials* (Eds: W. C. Connor, J. Fraissard), Springer, The Netherlands, **2006**, pp. 415–437.
[22] G. Freiman, J.-P. Korb, B. Nicot, P. Ligneul. *Diffus. Fundam.* **2009**, *10*, 25.1–25.3.
[23] J.-P. Korb, G. Freiman, B. Nicot, P. Ligneul. *Phys. Rev. E* **2009**, *80*, 061601-1–061601-12; DOI: 10.1103/PhysRevE.80.061601.
[24] G. Diakova, J.-P. Korb, R. G. Bryant. *Magn. Reson. Med.* **2012**, *68*, 272–277; DOI: 10.1002/mrm.23229.
[25] E. Rössler, C. Mattea, A. Mollova, S. Stapf. *J. Magn. Reson.* **2011**, *213*, 112–118; DOI: 10.1016/j.jmr.2011.09.014.
[26] B. R. R. Persson, L. Malmgren, L. G. Salford. *J. Bioeng. Biomed. Sci.* **2012**, *2*, 105; DOI: 10.4172/2155-9538.1000105.
[27] C. J. Hsieh, Y. W. Chen, D. W. Hwang. *Phys. Chem. Chem. Phys.* **2013**, *15*, 16634–16640; DOI: 10.1039/c3cp51739j.
[28] C. C. Fraenza, C. J. Meledandri, E. Anoardo, D. F. Brougham. *Chemphyschem* **2014**, *15*, 425–435; DOI: 10.1002/cphc.201301051.
[29] J.-P. Korb, R. G. Bryant. *Biophys. J.* **2005**, *89*, 2685–2692; DOI: 10.1529/biophysj.105.060178.
[30] D. S. Grebenkov, Y. A. Goddard, G. Diakova, J.-P. Korb, R. G. Bryant. *J. Phys. Chem. B* **2009**, *113*, 13347–13356; DOI: 10.1021/jp9048082.
[31] E. P. Sunde, B. Halle. *J. Am. Chem. Soc.* **2009**, *131*, 18214–18215; DOI: 10.1021/ja908144y.
[32] Y. A. Goddard, J.-P. Korb, R. G. Bryant. *J. Magn. Reson.* **2009**, *199*, 68–74; DOI: 10.1016/j.jmr.2009.04.001.
[33] E. Persson, B. Halle. *J. Am. Chem. Soc.* **2008**, *130*, 1774–1787; DOI: 10.1021/ja0775873.
[34] G. Diakova, Y. A. Goddard, J.-P. Korb, R. G. Bryant. *Biophys. J.* **2010**, *98*, 138–146; DOI: 10.1016/j.bpj.2009.09.054.
[35] G. Diakova, Y. Goddard, J.-P. Korb, R. G. Bryant. *J. Magn. Reson.* **2011**, *208*, 195–203; DOI: 10.1016/j.jmr.2010.11.001.
[36] S. Kariyo, S. Stapf. *Macromolecules* **2002**, *35*, 9253–9255; DOI: 10.1021/ma025632f.
[37] S. Kariyo, S. Stapf. *Solid State Nucl. Magn. Reson.* **2004**, *25*, 64–71; DOI: 10.1016/j.ssnmr.2003.03.011.
[38] S. Kariyo, A. Brodin, C. Gainaru, A. Herrmann, J. Hintermeyer, H. Schick, V. N. Novikov, E. A. Rössler. *Macromolecules* **2008**, *41*, 5322–5332; DOI: 10.1021/ma702758j.
[39] A. Gubaidullin, T. Shakirov, N. Fatkullin, R. Kimmich. *Solid State Nucl. Magn. Reson.* **2009**, *35*, 147–151; DOI: 10.1016/j.ssnmr.2008.10.004.
[40] N. Fatkullin, A. Gubaidullin, S. Stapf. *J. Chem. Phys.* **2010**, *132*, 094903-1–094903-17; DOI: 10.1063/1.3336832.
[41] E. A. Rössler, S. Stapf, N. Fatkullin. *Curr. Opin. Colloid Interface Sci.* **2013**, *18*, 173–182; DOI: 10.1016/j.cocis.2013.03.005.
[42] E. E. Burnell, D. Capitani, C. Casieri, A. L. Segre. *J. Phys. Chem. B* **2000**, *104*, 8782–8791; DOI: 10.1021/jp000691l.
[43] F. Bonetto, E. Anoardo, R. Kimmich. *J. Chem. Phys.* **2003**, *118*, 9037; DOI: 10.1063/1.1566735.
[44] P. J. Sebastião, D. Sousa, A. C. Ribeiro, M. Vilfan, G. Lahajnar, J. Seliger, S. Žumer. *Phys. Rev. E* **2005**, *72*, 061702; DOI: 10.1103/PhysRevE.72.061702.
[45] A. Gradišek, T. Apih, V. Domenici, V. Novotnad, P. José Sebastião. *Soft Matter* **2013**, *9*, 10746–10753; DOI: 10.1039/C3SM51625C.
[46] A. Plassaisa, M.-P. Pomies, N. Lequeux, P. Boch, J.-P. Korb, D. Petit, F. Barberon. *Magn. Reson. Imaging* **2003**, *21*, 369–371; DOI: 10.1016/S0730-725X(03)00141-3.
[47] P. J. McDonald, J.-P. Korb, J. Mitchell, L. Monteilhet. *Phys. Rev. E* **2005**, *72*, 011409-1–011409-9; DOI: 10.1103/PhysRevE.72.011409.
[48] J.-P. Korb, L. Monteilhet, P. J. McDonald, J. Mitchell. *Cement Concr. Res.* **2007**, *37*, 295–302; DOI: 10.1016/j.cemconres.2006.08.002.
[49] S. Haber-Pohlmeier, S. Stapf, D. van Dusschoten, A. Pohlmeier. *Open Magn. Reson. J.* **2010**, *3*, 57–62.
[50] G. E. Schaumann, D. Diehl, M. Bertmer, A. Jaeger, P. Conte, G. Alonzo, J. Bachmann. *J. Hydrol. Hydromech.* **2013**, *61*, 50–63; DOI: 10.2478/johh-2013-0007.
[51] P. Conte, G. Alonzo. *eMagRes* **2013**, *2*, 389–398; DOI: 10.1002/9780470034590.emrstm1330.
[52] P. Conte, U. M. Hanke, V. Marsala, G. Cimò, G. Alonzo, B. Glaser. *J. Agric. Food Chem.* **2014**, *62*, 4917–4923; DOI: 10.1021/jf5010034.
[53] S. Stapf, X. Ren, E. Talnishnikh, B. Blümich. *Magn. Reson. Imaging* **2005**, *23*, 383–386; DOI: 10.1016/j.mri.2004.11.036.
[54] S. Godefroy, J. P. Korb, L. K. Creamer, P. J. Watkinson, P. T. Callaghan. *J. Colloid Interface Sci.* **2003**, *267*, 337–342; DOI: 10.1016/S0021-9797(03)00589-7.
[55] D. Capitani, A. P. Sobolev, M. Delfini, S. Vista, R. Antiochia, N. Proietti, S. Bubici, G. Ferrante, S. Carradori, F. R. De Salvador, L. Mannina. *Electrophoresis* **2014**, *35*, 1615–1626; DOI: 10.1002/elps.201300629.
[56] S. Baroni, R. Consonni, G. Ferrante, S. Aime. *J. Agric. Food Chem.* **2009**, *57*, 3028–3032; DOI: 10.1021/jf803727d.
[57] M. Lévy, F. Gazeau, C. Wilhelm, S. Neveu, M. Devaud, P. Levitz. *J. Phys. Chem. C* **2013**, *117*, 15369–15374; DOI: 10.1021/jp404199f.
[58] C. de Cola, G. Fiorillo, A. Meli, S. Aime, E. Gianolio, I. Izzo, F. De Riccardis. *Org. Biomol. Chem.* **2014**, *12*, 424–431; DOI: 10.1039/c3ob42029a.
[59] T. Borase, T. Ninjbadgar, A. Kapetanakis, S. Roche, R. O'Connor, C. Kerskens, A. Heise, D. F. Brougham. *Angew. Chem. Int. Ed.* **2013**, *52*, 3164–3167; DOI: 10.1002/anie.201208099.
[60] R. R. Regatte, S. V. S. Akella, J. H. Lonner, J. B. Kneeland, R. Reddy. *J. Magn. Reson. Imaging* **2006**, *23*, 547–553; DOI: 10.1002/jmri.20536.
[61] J.-P. Korb, M. Whaley, R. G. Bryant. *Phys. Rev. E* **1997**, *56*, 1934–1945; DOI: 10.1103/PhysRevE.56.1934.

Copyright © 2015 John Wiley & Sons, Ltd.

[62] J.-P. Korb, A. Louis-Joseph, L. Benamsili. *J. Phys. Chem. B* **2013**, *117*, 7002–7014; DOI: 10.1021/jp311910t.
[63] L. Zielinski, M. D. Hurlimann. *Energ. Fuel* **2011**, *25*, 5090–5099; DOI: 10.1021/ef20088.
[64] M. Gottschalk, K. Venu, B. Halle. *Biophys. J.* **2003**, *84*, 3941–3958; DOI: 10.1016/S0006-3495(03)75122-4.
[65] E. P. Sunde, B. Halle. *J. Magn. Reson.* **2010**, *203*, 257–273; DOI: 10.1016/j.jmr.2010.01.008.
[66] L. M. Broche, S. R. Ismail, N. A. Booth, D. J. Lurie. *Magn. Reson. Med.* **2012**, *67*, 1453–1457; DOI: 10.1002/mrm.23117.
[67] S. Bubici, R. Steele, G. Ferrante. Fast field cycling relaxometry: moving from research towards industrial applications. *Proceedings of the 54th Experimental Nuclear Magnetic Resonance Conference*, poster abstract, Asilomar, USA; 14–19 April **2013**.
[68] L. Laghi, M. A. Cremonini, G. Placucci, S. Sykora, K. Wright, B. Hills. *Magn. Reson. Imaging* **2005**, *23*, 501–510; DOI: 10.1016/j.mri.2004.12.003.
[69] E. Curti, S. Bubici, E. Carini, S. Baroni, E. Vittadini. *LWT-Food Sci. Technol.* **2011**, *44*, 854–859; DOI: 10.1016/j.lwt.2010.11.021.
[70] P. Conte, V. Mineo, S. Bubici, C. De Pasquale, F. Aboud, A. Maccotta, D. Planeta, G. Alonzo. *Anal. Bioanal. Chem.* **2011**, *400*, 1443–1450; DOI: 10.1007/s00216-011-4904-8.
[71] G. Ferrante, S. Bubici, J.-P. Korb, M. Mallett. Poster communication, "New technology and an instrumental platform for the exploitation of the field-dependence of T_1 and T_2 in rock core analysis and petroleum applications." *Proceedings of the 12th International Bologna Conference on Magnetic Resonance in Porous Media (MRPM12)*, poster abstract, Wellington, New Zealand; 9–13 February **2014**.
[72] J. K. Alford, B. K. Rutt, T. J. Scholl, W. B. Handler, B. A. Chronik. *Magn. Reson. Med.* **2009**, *61*, 796–802; DOI: 10.1002/mrm.21933.
[73] M. D. Hürlimann, L. Venkataramanan. *J. Magn. Reson.* **2002**, *157*, 31–42; DOI: 10.1006/jmre.2002.2567.
[74] A. R. Mutina, M. D. Hürlimann. *J. Phys. Chem. A* **2008**, *112*, 3291–3301; DOI: 10.1021/jp710254d.
[75] N. Marigheto, L. Venturi, D. Hibberd, K. M. Wright, G. Ferrante, B. P. Hills. *J. Magn. Reson.* **2007**, *187*, 327–342; DOI: 10.1016/j.jmr.2007.04.016.
[76] J.-P. Korb, B. Nicot, A. Louis-Joseph, S. Bubici, G. Ferrante. *J. Phys. Chem. C* **2014**, *118*, 23212–23218; DOI: 10.1021/jp508659e.

Copyright © 2015 John Wiley & Sons, Ltd.